BIOCHEMISTRY
including biophysical chemistry & molecular biology
Article

Biochemistry **2010,** *49,* 10089–10097 10089
DOI: 10.1021/bi101020p

Photosensitivities of Rhodopsin Mutants with a Displaced Counterion[†]

Kei Tsutsui[‡] and Yoshinori Shichida*

Department of Biophysics, Graduate School of Science, Kyoto University, Kyoto 606-8502, Japan.
[‡]Present address: Graduate School of Frontier Biosciences, Osaka University, Suita, Osaka 565-0871, Japan.

Received June 25, 2010; Revised Manuscript Received October 5, 2010

ABSTRACT: Visual pigments consist of a protein moiety opsin and an 11-*cis*-retinal chromophore that is covalently bound to the opsin via a Schiff base linkage. They have a high photosensitivity, which can be attributed to the high probability of photon absorption and the high photoisomerization quantum yield of the retinal chromophore. Both of these parameters are regulated by the opsin, though the precise mechanism is unknown. We previously found that counterion residue E113, which stabilizes the proton on the Schiff base, is involved in the efficient photoisomerization in vertebrate visual pigments. To test the positional effect of the counterion on the photon absorption and the photoisomerization, we measured the photosensitivities of a set of mutants of bovine rhodopsin in which the counterion was displaced to position 90, 94, 117, or 292. The molar extinction coefficient was reduced in many of the mutants, leading to reductions in the photosensitivity for monochromatic lights. However, the oscillator strength, the probability of photon absorption integrated over the entire wavenumber range of the absorption band, was relatively similar among the mutants and the wild type. In addition, the quantum yields of the mutants were not markedly different from that of the wild type. These results indicate that the counterion does not need to be located at position 113 for a high photosensitivity for natural light. Interestingly, all of the mutants exhibited greatly increased hydroxylamine sensitivity. This result suggests that the counterion in vertebrate visual pigments is optimally located for the stability of the Schiff base linkage.

Visual pigments are photosensitive molecules in photoreceptor cells and consist of a protein moiety opsin and an 11-*cis*-retinal chromophore that is covalently bound to the opsin via a Schiff base linkage. The chromophore becomes excited upon photon absorption and undergoes a quite efficient *cis*−*trans* photoisomerization reaction (*1*). The photoisomerization triggers a conformational change in the opsin and activation of the G protein-mediated phototransduction cascade, which eventually leads to hyperpolarization of the photoreceptor cell (*2*). Thus, the probability of photon absorption and the photoisomerization efficiency (quantum yield) of a visual pigment directly affect the photosensitivity of the photoreceptor cell.

Most visual pigments, including rhodopsins, absorb maximally in the visible region of light. The visible light sensitivity is achieved by protonation of the Schiff base of the retinal chromophore. The protonated Schiff base is stabilized by an amino acid residue called the "counterion" (*3*). In vertebrate visual pigments, E113[1] acts as the Schiff base counterion (*4*−*6*). E113 is also conserved in UV-absorbing visual pigments that have an unprotonated chromophore.

We previously found that E113 is required for efficient photoisomerization in mouse UV[2] cone pigment and probably in chicken violet and bovine rhodopsin (*7*, *8*). That discovery raised a question. Is E113 optimally located for photoisomerization efficiency, or can a counterion at another position(s) also facilitate photoisomerization? This is not only an interesting issue in terms of protein photochemistry but also an important question in terms of understanding the mechanism of functional differences between vertebrate visual pigments and invertebrate rhodopsins, which do not have E113 but rather E181 as the Schiff base counterion (*9*).

In this study, we explored the positional effect of the Schiff base counterion on the photosensitivity of rhodopsin. A set of mutants of bovine rhodopsin in which the counterion was displaced was generated: E113 was neutralized by a mutation (E113Q or E113A), and glutamate or aspartate was introduced at another position near the Schiff base that has been shown or suggested to be able to be the counterion site [position 90 (*10*), 94 (*11*), 117 (*12*, *13*), or 292 (*14*)] (Figure 1A). The E113D mutant was also generated. The molar extinction coefficient was reduced in many of the mutants, leading to reductions in the photosensitivity for monochromatic lights. However, the oscillator strength, the probability of photon absorption integrated over the entire wavenumber range of the absorption band, was relatively similar among the mutants and the wild type. In addition, the quantum yields of the mutants were not markedly different from that of the wild type. These results indicate that the counterion does not need to be located at position 113 for a high photosensitivity for natural light. Interestingly, however, all of the mutants but E113D exhibited greatly increased hydroxylamine sensitivity. This result suggests that position 113 is the optimal counterion location for the stability of the Schiff base linkage.

[†]This work was supported in part by Grants-in-Aid for Scientific Research on Priority Areas (21027090) and for Scientific Research (S) (20227002) and a Grant for the Global Center of Excellence Program (A6) from the Japanese Ministry of Education, Culture, Sports, Science, and Technology to Y.S. K.T. was supported by the Japanese Society for the Promotion of Science Research Fellowships for Young Scientists.

*To whom correspondence should be addressed. Telephone: +81-75-753-4213. Fax: +81-75-753-4210. E-mail: shichida@rh.biophys.kyoto-u.ac.jp.

[1]The numbers of all amino acid residues in this paper are based on the bovine rhodopsin numbering system.

[2]Abbreviations: UV, ultraviolet; DM, dodecyl β-D-maltoside; HEPES, *N*-(2-hydroxyethyl)piperazine-*N*′-2-ethanesulfonic acid; λ_{max}, wavelength at the absorption maximum; HPLC, high-performance liquid chromatography; PDB, Protein Data Bank.

Published on Web 11/01/2010

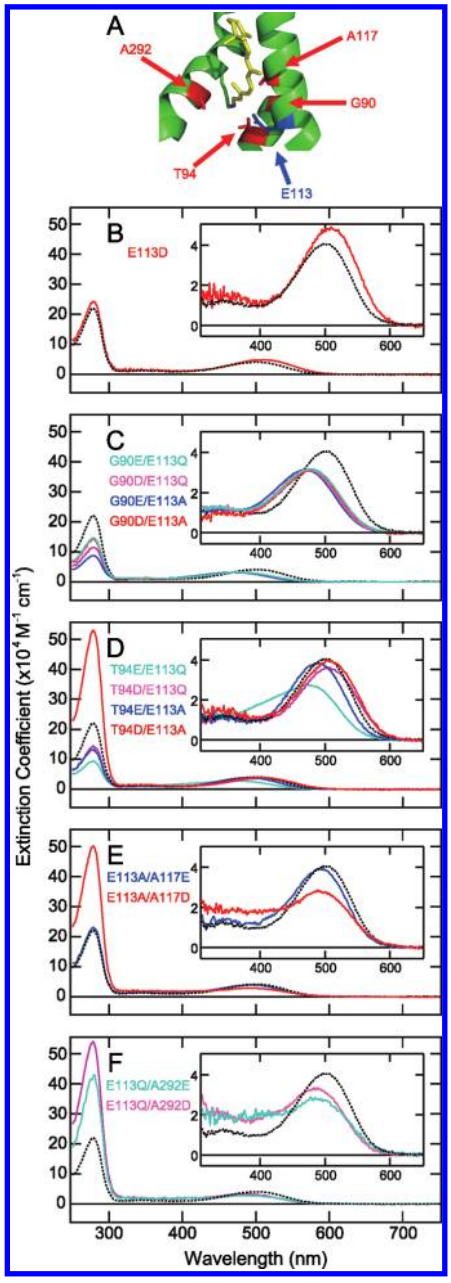

FIGURE 1: (A) Partial view of the bovine rhodopsin structure (PDB entry 1U19) (*20*) showing the amino acid positions at which counterions were introduced. Glutamate or asparatate was introduced at one of the indicated sites [G90, T94, A117, or A292 (red)], and E113 (blue) was neutralized by an E113Q or E113A mutation. The E113D mutant was also generated. The retinal chromophore and the Schiff base nitrogen are colored yellow and blue, respectively. (B−F) Absorption spectra of the mutants. Molar extinction coefficients were determined by the acid denaturation method. The λ_{max} values are summarized in Table 1. In each panel, the absorption spectra of the mutants are shown in different colors, and the absorption spectrum of the wild type is shown as a dotted line. An expanded view of the λ_{max} band is shown as an inset in each panel: (B) E113D, (C) G90E/E113Q, G90D/E113Q, G90E/E113A, and G90D/E113A, (D) T94E/E113Q, T94D/E113Q, T94E/E113A, and T94D/E113A, (E) E113A/A117E and E113A/A117D, and (F) E113Q/A292E and E113Q/A292D.

MATERIALS AND METHODS

Sample Preparation. The cDNAs of wild-type and mutant bovine rhodopsin were introduced into an expression vector, pcDNA3.1 (Invitrogen) or pUSRα (*15*). The cDNAs of site-directed mutants were constructed using the QuikChange mutagenesis kit (Stratagene). The wild-type and mutant opsins were expressed in the HEK 293T cell line and regenerated with 11-*cis*-retinal as previously reported (*16*). The reconstituted pigments were extracted with buffer A [1% (w/v) DM, 25 mM HEPES, 70 mM NaCl, and 1.5 mM $MgCl_2$ (pH 6.5) at 3 °C] and purified by adsorption on an antibody-conjugated column and elution with buffer B [0.3 mg/mL 1D4 peptide, 0.02% DM, 50 mM HEPES, 140 mM NaCl, and 3 mM $MgCl_2$ (pH 6.5)], unless noted otherwise.

Molar Extinction Coefficient. The molar extinction coefficients were determined relative to that of wild-type bovine rhodopsin [40600 M^{-1} cm^{-1} (*17*)] by the acid denaturation method, as previously described (*7*).

Oscillator Strength. Oscillator strengths were calculated according to the method of Birge et al. (*18*). Briefly, the absorption spectra in the wavenumber scale were fitted with a log-normal function (described in ref *18*) from 16393 to 22472 cm^{-1}, and coefficients "full width at half-maximum" and "skewness (measure of asymmetry)" were obtained. Then the oscillator strength was calculated using the values according to the reference.

HPLC Analysis. HPLC analysis was performed as described previously, with some modifications (*7*). A sample containing rhodopsin was divided into two aliquots. One was kept in the dark, and the other was irradiated at 3 °C in the presence of hydroxylamine (the final concentration of hydroxylamine was 480 μM except as follows: 48 mM for the wild type, E113D, and E113A/A117E and 48 μM for G90E/E113Q and G90D/E113Q). For irradiation, light from a 1 kW tungsten lamp (Master HILUX-HR, Rikagaku) that had been passed through an interference filter (500 nm; half-bandwidth, 5 nm; Optical Coatings Japan) was used. Then the chromophores were extracted as retinaloximes and subjected to HPLC analysis. Using the result of the HPLC analysis, the percentages of isomers (9-*cis*, 11-*cis*, 13-*cis*, and all-*trans*) were determined for the dark and irradiated samples.

Photosensitivity. The photosensitivities of the rhodopsin mutants were determined by UV−vis spectrophotometry using a Hitachi U-4100 spectrophotometer as previously described (*7*). Briefly, the sample was successively irradiated by 500 nm light at 3 °C in the presence of hydroxylamine (light and the concentrations of hydroxylamine were the same as those described above). Finally, the sample was completely bleached with > 500 nm light (VY52 filter, Toshiba) to define the baseline. The absorbance change was monitored at the respective λ_{max} of the minus-baseline difference spectra. The amounts of residual pigment at each step of irradiation were determined from the absorbances after correction for hydroxylamine bleaching (see the Supporting Information of ref *7*), plotted on a semilogarithmic scale against the incident photon number, and fitted to a single-exponential function. The slope of the fitting line relative to that of the wild-type bovine rhodopsin when irradiated at 500 nm was defined as the photosensitivity of the pigment at 500 nm. Then the photosensitivity at λ_{max} was calculated using the ratio of the extinction coefficient at 500 nm and at λ_{max}. Here the photosensitivity is a relative, unitless number. It should be noted that what we directly measured was the light-dependent formation of hydroxylamine-reactive species, not photoisomerization. However, the formation of hydroxylamine-reactive species should correspond to photoisomerization on the reasonable assumptions that hydroxylamine reactivity increases only when the chromophore photoisomerizes and photoisomerization always involves an increase in hydroxylamine reactivity.

Table 1: Spectroscopic Properties of the Rhodopsin Mutants

pigment	λ_{max}[a] (nm)	ε_{max}[b] (M^{-1} cm^{-1})	fwhm[c] (cm^{-1})	f[d]
wild type	500	40600[e] (1.00)[f]	4120 (1.00)	0.79 (1.00)
E113D	508	48400 ± 1000[g] (1.19 ± 0.03)	4120 (1.00)	0.94 ± 0.02 (1.19 ± 0.02)
G90E/E113Q	477	31800 ± 1600 (0.78 ± 0.04)	4900 (1.19)	0.73 ± 0.04 (0.93 ± 0.05)
G90D/E113Q	473	31400 ± 1500 (0.77 ± 0.04)	4870 (1.18)	0.72 ± 0.03 (0.91 ± 0.04)
G90E/E113A	469	31500 ± 1500 (0.77 ± 0.04)	5080 (1.23)	0.75 ± 0.04 (0.95 ± 0.04)
G90D/E113A	477	30900 ± 1900 (0.76 ± 0.05)	4850 (1.18)	0.71 ± 0.04 (0.89 ± 0.05)
T94E/E113Q	473	27000 ± 1600[g] (0.67 ± 0.04)	5470 (1.33)	0.71 ± 0.04 (0.90 ± 0.05)
T94D/E113Q	505	36000 ± 900 (0.89 ± 0.02)	4280 (1.04)	0.72 ± 0.02 (0.92 ± 0.02)
T94E/E113A	488	38400 ± 800 (0.95 ± 0.02)	4380 (1.06)	0.79 ± 0.02 (1.00 ± 0.02)
T94D/E113A	506	39500 ± 900 (0.97 ± 0.02)	4310 (1.04)	0.80 ± 0.02 (1.02 ± 0.02)
E113A/A117E	492	39200 ± 2000 (0.96 ± 0.05)	4290 (1.04)	0.79 ± 0.04 (1.00 ± 0.05)
E113A/A117D	491	28000 ± 900[h] (0.69 ± 0.02)	5020 (1.22)	0.66 ± 0.02 (0.84 ± 0.03)
E113Q/A292E	487	28100 ± 1600[h] (0.69 ± 0.04)	5060 (1.23)	0.67 ± 0.04 (0.85 ± 0.05)
E113Q/A292D	484	33000 ± 1700[h] (0.81 ± 0.04)	4970 (1.21)	0.78 ± 0.04 (0.98 ± 0.05)

[a]Wavelength at the absorption maximum. [b]Molar extinction coefficient at λ_{max}. [c]Full width at half-maximum. [d]Oscillator strength of the λ_{max} band. [e]From ref *17*. [f]The values in parentheses are values relative to the wild type. [g]The effect of the presence of the isomers other than 11-*cis*-retinal in the binding pocket is not considered. [h]The effect of the possible presence of the unprotonated form is not considered.

Quantum Yield. The quantum yields (φ) of visual pigments were calculated using the following relationship (*7*):

$$S \propto \varepsilon\varphi$$

where S and ε are the photosensitivity at 500 nm (relative to the wild type) and the molar extinction coefficient at 500 nm, respectively. This formula, together with the molar extinction coefficient of the wild type at 500 nm [40600 M^{-1} cm^{-1} (*17*)], gives us the quantum yields relative to the wild type. Then the absolute values of quantum yields were determined using the value of the wild type [0.65 (*19*)].

Hydroxylamine Sensitivity. The hydroxylamine sensitivities of the rhodopsin mutants were determined as the rate constants of dark bleaching at 3 °C in the presence of 480 μM hydroxylamine. When the final concentration of hydroxylamine was 48 mM or 48 μM, values at 480 μM were determined by multiplying the measured value by 0.01 or 10, respectively.

Molecular Modeling. Molecular modeling was performed using the molecular operating environment (MOE) software package (Chemical Computing Group Inc.). The crystal structure of bovine rhodopsin (PDB entry 1U19) (*20*) was used as a template. First, the E113Q or E113A mutation was introduced. When the E113Q mutation was introduced, sterically possible rotamers of Q113 were generated and the rotamer that was the most similar to the rotamer of E113 in the wild type was adopted. Then glutamate or aspartate was introduced at position 90, 94, 117, or 292, and sterically possible rotamers of the introduced amino acid were generated. The rotamer that gave the shortest distance between the two oxygen atoms of the introduced carboxylic acid and the Schiff base nitrogen was adopted.

RESULTS

Absorption Spectra. Bovine rhodopsin mutants with a displaced counterion were generated, and the absorption spectra were measured (Figure 1). All of the mutants had their λ_{max} values in the visible region, but some of them (E113A/A117D, E113Q/A292E, and E113Q/A292D) exhibited a broad UV absorbance (300−400 nm) (Figure 1E,F). This might be derived from either a subfraction with an unprotonated Schiff base generated by a lowering of the Schiff base pK_a, the β band with an increased intensity, or some impurity that had a relatively strong contribution because of the low expression level of the mutants. On the basis of the first possibility, we tried to eliminate the UV-absorbing species by lowering the sample pH to 5 in the mutants, but the absorption spectra were not much changed (data not shown). Further lowering of the pH was difficult because of denaturation of the proteins. The absorption spectrum of T94E/E113Q showed a unique shoulder around 400 nm (Figure 1D). The mutants showed a variety of λ_{max} values (469−508 nm) (Table 1), suggesting that interactions between the Schiff base and the counterion were different among different mutants. The λ_{max} values of mutants G90D/E113Q, G90D/E113A, E113D, and E113A/A117E were almost identical to previously reported values (*4*, *5*, *10*, *21*, *22*). On the other hand, the T94D/E113Q mutant had a λ_{max} at 505 nm, which is notably different from a previously reported value, 490 nm (*23*). Changing the sample pH from 6.5 (our condition) to 8.0 (the reported condition) caused partial formation of the unprotonated form but no spectral shift of the protonated form (data not shown). It is not clear why we could not reproduce the reported result. The mutants exhibited various ratios of absorbance at 280 nm to that at λ_{max} (Figure 1B−F), suggesting that some mutations affected the efficiency of protein folding and/or chromophore binding.

Molar Extinction Coefficients, Bandwidths, and Oscillator Strengths. The molar extinction coefficients of the mutants were determined by the acid denaturation method (*7*). The molar extinction coefficients at the respective λ_{max} values are shown in Figure 2A and listed in Table 1. Many of the mutants exhibited reduced extinction coefficients compared with that of the wild type (67−81%). On the other hand, the extinction coefficients of some mutants (T94D/E113Q, T94E/E113A, T94D/E113A, and E113A/A117E) were similar to that of the wild type (89−97%). The E113D mutant showed a higher extinction coefficient than the wild type (119%). It cannot be denied that the values for the E113A/A117D, E113Q/A292E, and E113Q/A292D mutants might be underestimated because of the possible presence of the unprotonated form. In addition, the values for the E113D and T94E/E113Q mutants contain some uncertainties because of the presence of isomers other than 11-*cis*-retinal in the binding pocket (described later).

At the same time, bandwidths (full widths at half-maximum) were affected by the location of the counterion (Figure 2B and Table 1). Interestingly, all of the mutants with a lower extinction

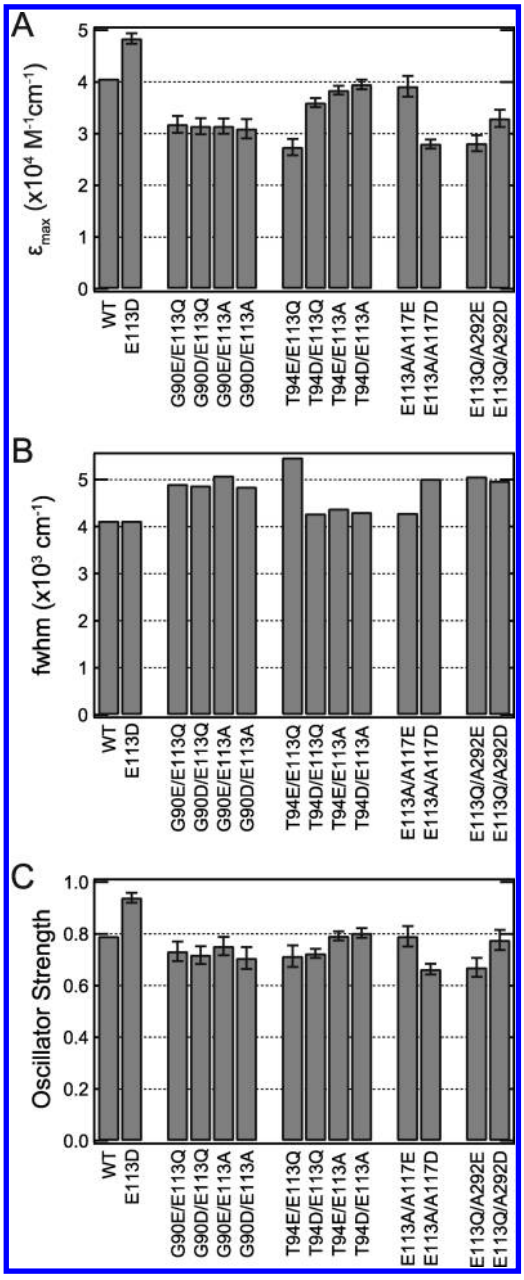

FIGURE 2: (A) Molar extinction coefficients (determined by the acid denaturation method) of the rhodopsin wild type and mutants at λ_{max}. The value for the wild type is from ref *17*. The values for the E113D, T94E/E113Q, E113A/E117D, E113Q/A292E, and E113Q/A292D mutants contain some uncertainties because of the presence of isomers other than 11-*cis*-retinal in the binding pocket (E113D and T94E/E113Q) or the possible presence of the unprotonated form (E113A/E117D, E113Q/A292E, and E113Q/A292D) (see the text). The values are also summarized in Table 1. (B) Full widths at half-maximum of the λ_{max} band (obtained by the fitting with a log-normal function) of the rhodopsin wild type and mutants. The values are also summarized in Table 1. (C) Oscillator strengths of the λ_{max} band (calculated using parameters obtained by the fitting) of the rhodopsin wild type and mutants. The values are also summarized in Table 1.

coefficient (67−81%) had a broadened bandwidth (118−133%), whereas all of the mutants with a wild-type-like extinction coefficient (89−119%) had a wild-type-like bandwidth (100−106%).

The molar extinction coefficient indicates the probability of photon absorption at a single wavelength. Probably more relevant to absorption probability for natural light with a broad spectrum is oscillator strength. Oscillator strength is a measure of electronic transition probability integrated over the entire range of an absorption band, and it can be calculated from an absorption spectrum plotted on the wavenumber scale with a known molar extinction coefficient (*18*). The calculated oscillator strengths of the α band (λ_{max} band) in the wild type and the mutants are shown in Figure 2C and listed in Table 1. In contrast to the pattern of the extinction coefficients, the oscillator strengths were relatively similar among the wild type and the mutants (84−119%). This is because the lower extinction coefficients in some of the mutants are compensated by the broadened bandwidths.

Isomeric Compositions of the Chromophore in the Dark State and the Photoproduct. In wild-type bovine rhodopsin, the binding pocket accommodates exclusively 11-*cis*-retinal and photoisomerization of 11-*cis*-retinal generates exclusively all-*trans*-retinal. To investigate whether it is also the case for the mutants, HPLC analysis of the dark states and the photoproducts was performed.

In the dark state, the chromophore in the mutants was almost exclusively (greater than ∼90%) 11-*cis*-retinal (data not shown) as in the case for the wild type (Figure 3A), except for the T94E/E113Q and E113D mutants. The dark state of the T94E/E113Q mutant contained a significant amount (30%) of all-*trans*-retinal along with 11-*cis*-retinal (data not shown). In the chromatogram of E113D, there was an unassignable peak that slightly preceded that of all-*trans*-15-*syn*-retinaloxime and a peak apparently corresponding to 13-*cis*-15-*anti*-retinaloxime, along with peaks for 11-*cis*-retinal (Figure 3A,B).

In the irradiated samples of the mutants, the photoproducts consisted almost exclusively (greater than ∼90%) of all-*trans*-retinal (data not shown) as in the case of the wild type (Figure 3A), except for the E113D mutant. In the E113D mutant, unexpectedly, the photoproducts contained a substantial amount of 13-*cis*-retinal along with all-*trans*-retinal (Figure 3A).

The results described above demonstrate that the isomeric composition of the dark state and the bond specificity of photoisomerization in all of the mutants but two are almost identical to those in the wild type. It should be noted that the molar extinction coefficients of the E113D and T94E/E113Q mutants determined by the acid denaturation method (Figure 2A and Table 1) might be incorrect because of the presence of the unidentified isomer and all-*trans*-retinal, respectively. The E113D mutant was excluded from the following photosensitivity measurements because it was difficult to determine the 11-*cis* to all-*trans* photosensitivity by UV−vis spectroscopy when the 13-*cis*-retinal photoproduct was generated at the same time.

Photosensitivities. The photosensitivities of the mutants relative to that of the wild type were measured by 500 nm irradiation in the presence of 48 μM, 480 μM, or 48 mM hydroxylamine. The concentration of hydroxylamine was selected so that the dark state was sufficiently stable and photointermediates did not persist, and corrections were made for dark bleaching (*7*).

The photosensitivities at the respective λ_{max} (calculated using the ratio of the extinction coefficient at 500 nm and at the respective λ_{max}) are shown in Figure 4A and listed in Table 2. Many of the mutants exhibited reduced photosensitivity relative to that of the wild type (61−83%). On the other hand, the photosensitivities of the T94D/E113A and E113A/A117E mutants were similar to that of the wild type (96−98%).

Quantum Yields. The quantum yields were calculated from the experimentally determined molar extinction coefficients at λ_{max} and photosensitivities at λ_{max} (Figure 4B and Table 2). The quantum yields of the mutants were similar to each other and to that of the wild type (88−104%). These results indicate that

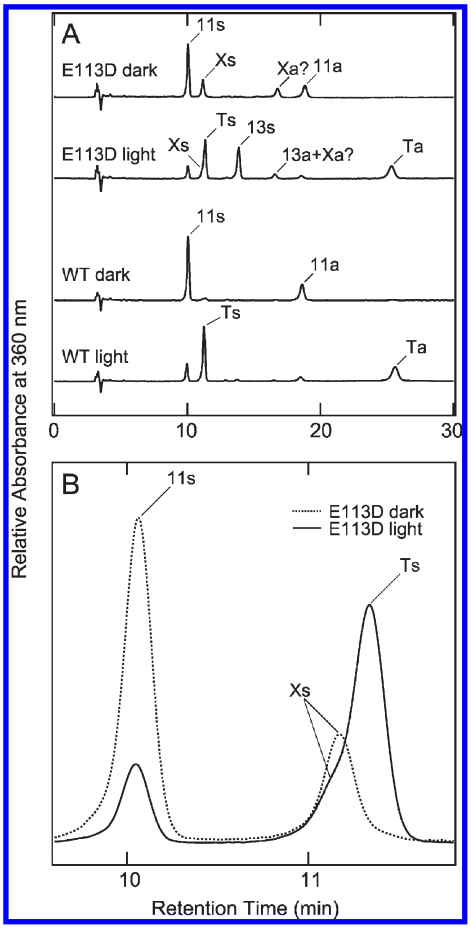

FIGURE 3: (A) HPLC analysis of the dark and irradiated states of the E113D mutant and the wild type (WT). Abbreviations: 11s, 11-*cis*-15-*syn*-retinaloxime; Ts, all-*trans*-15-*syn*-retinaloxime; 13s, 13-*cis*-15-*syn*-retinaloxime; Xs, 15-*syn*-retinaloxime of the unidentified isomer; 11a, 11-*cis*-15-*anti*-retinaloxime; Ta, all-*trans*-15-*anti*-retinaloxime; 13a, 13-*cis*-15-*anti*-retinaloxime; Xa, 15-*anti*-retinaloxime of the unidentified isomer. We speculated that Xa had a retention time identical to that of 13a. (B) Expanded view of the HPLC chromatograms of the dark (---) and irradiated (—) states of the E113D mutants. The peak of Xs had a retention time similar to but distinct from that of Ts.

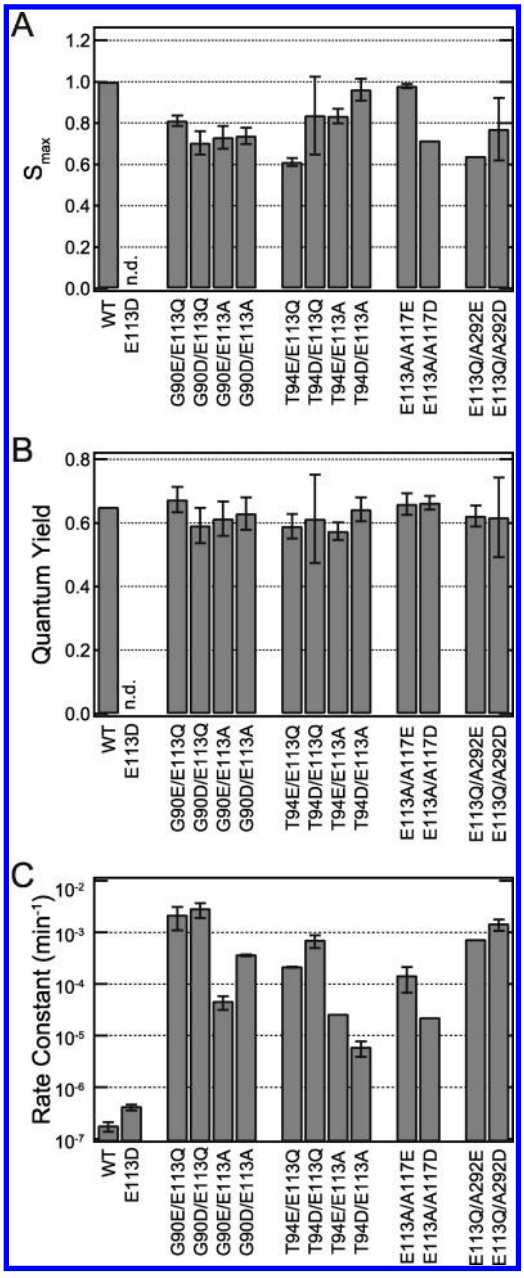

FIGURE 4: (A) Photosensitivities of the rhodopsin wild type and mutants (relative to that of the wild type) at λ_{max} that were calculated from the photosensitivities at 500 nm. The value for the E113D mutant was not determined (denoted as n.d.). The values are also summarized in Table 2. (B) Quantum yields of the rhodopsin wild type and mutants that were calculated from the experimentally determined molar extinction coefficients and the photosensitivities at 500 nm. The value for the wild type is from ref *19*. The value for the E113D mutant was not determined (denoted as n.d.). The values are also summarized in Table 2. (C) Hydroxylamine sensitivity of the rhodopsin wild type and mutants on a logarithmic scale. The rate constant of bleaching was measured at 3 °C in the presence of 480 μM hydroxylamine. The values are also summarized in Table 2.

a counterion that is located at positions other than position 113 can facilitate photoisomerization of the chromophore. Together with the finding that oscillator strengths are not largely affected in the mutants, we can conclude that the counterion does not need to be located at position 113 for a high photosensitivity for natural light.

Hydroxylamine Sensitivities. In the course of the photosensitivity measurements, it turned out that all of the mutants but E113D are highly susceptible to hydroxylamine. There were ~100−10000-fold increases in the rate constant of dark bleaching at 3 °C in the presence of 480 μM hydroxylamine (Figure 4C and Table 2). It was previously reported that the G90D/E113A mutant exhibited increased hydroxylamine sensitivity (*21*). These results suggest that position 113 is the optimal counterion location for the stability of the Schiff base linkage.

Molecular Modeling. To quantitatively understand the relationship between the location of the counterion and the extinction coefficient of the rhodopsin mutants, molecular modeling was performed. First, the E113Q or E113A mutation was introduced into the bovine rhodopsin structure (PDB entry 1U19) (*20*). When the E113Q mutation was introduced, sterically possible rotamers of Q113 were generated and the rotamer that was the most similar to the rotamer of E113 in the wild type was adopted. Then glutamate or aspartate was introduced at position 90, 94, 117, or 292, and sterically possible rotamers of the introduced amino acid were generated. The rotamer that gave the shortest distance between the two oxygen atoms of the introduced carboxylic acid and the Schiff base nitrogen was adopted, because a salt bridge between the counterion and the Schiff base would favor the shortest distance. Here amino acid residues other than

Table 2: Reactive Properties of the Rhodopsin Mutants

pigment	S_{max} [a]	φ [b]	k_{NH_2OH} [c] (min^{-1})
wild type	1.00	0.65 [d] (1.00)	$(1.7 \pm 0.4) \times 10^{-7}$ (1.00)
E113D	not determined	not determined	$(4.1 \pm 0.5) \times 10^{-7}$ (2.4 ± 0.3)
G90E/E113Q	0.81 ± 0.03	0.67 ± 0.04 (1.04 ± 0.06)	$(2.1 \pm 1.0) \times 10^{-3}$ (12000 ± 6000)
G90D/E113Q	0.70 ± 0.06	0.59 ± 0.06 (0.91 ± 0.08)	$(2.8 \pm 0.9) \times 10^{-3}$ (16000 ± 5000)
G90E/E113A	0.73 ± 0.06	0.61 ± 0.05 (0.94 ± 0.08)	$(4.4 \pm 1.3) \times 10^{-5}$ (250 ± 80)
G90D/E113A	0.74 ± 0.04	0.63 ± 0.05 (0.97 ± 0.08)	$(3.6 \pm 0.1) \times 10^{-4}$ (2100 ± 70)
T94E/E113Q	0.61 ± 0.02	0.59 ± 0.04 (0.91 ± 0.06)	$(2.1 \pm 0.0) \times 10^{-4}$ (1200 ± 20)
T94D/E113Q	0.83 ± 0.19	0.61 ± 0.14 (0.94 ± 0.21)	$(6.7 \pm 2.0) \times 10^{-4}$ (3900 ± 1100)
T94E/E113A	0.83 ± 0.04	0.57 ± 0.03 (0.88 ± 0.04)	3.4×10^{-4} (140)
T94D/E113A	0.96 ± 0.05	0.64 ± 0.04 (0.99 ± 0.06)	$(5.8 \pm 1.9) \times 10^{-5}$ (33 ± 11)
E113A/A117E	0.98 ± 0.01	0.66 ± 0.03 (1.01 ± 0.05)	$(1.7 \pm 0.4) \times 10^{-4}$ (810 ± 420)
E113A/A117D	0.72	0.66 ± 0.02 (1.02 ± 0.03)	2.2×10^{-5} (120)
E113Q/A292E	0.64	0.62 ± 0.03 (0.96 ± 0.05)	7.1×10^{-4} (4000)
E113Q/A292D	0.77 ± 0.15	0.62 ± 0.13 (0.95 ± 0.19)	$(1.4 \pm 0.4) \times 10^{-3}$ (8200 ± 2100)

[a]Photosensitivity at λ_{max} (relative to that of the wild type). [b]Quantum yield. [c]Rate constant of bleaching at 3 °C in the presence of 480 μM hydroxylamine. [d]From ref *19*.

the introduced one were assumed to be fixed. Although this assumption may not be strictly valid, the modeling offered clear and reasonable results (Figure 5). In the mutants with a wild-type-like extinction coefficient (89−119%) and a wild-type-like bandwidth (100−106%), the counterions are located approximately in the plane that contains the 13-methyl group and the Schiff base region of the retinal chromophore (Figure 5A). In contrast, in the mutants with a lower extinction coefficient (67−81%) and a broader bandwidth (118−133%), the counterions are located out of this plane (Figure 5B). There was no correlation between the counterion−Schiff base distance and the extinction coefficient (data not shown).

DISCUSSION

Advantage of Having the Counterion at Position 113. In this study, we measured the molar extinction coefficients, oscillator strengths, photosensitivities, and quantum yields of bovine rhodopsin mutants with a displaced counterion. The quantum yields of the mutants were similar to that of the wild type (88−104%) (Figure 4B and Table 2), indicating that a counterion that is located at positions other than position 113 can facilitate photoisomerization of the chromophore. In other words, the counterion does not have to be located at position 113 to facilitate photoisomerization efficiency.

The molar extinction coefficient, in contrast, was reduced in many of the mutants (67−81%) (Figure 2A and Table 1). However, some mutants exhibited molar extinction coefficients that were similar to that of the wild type (89−97%), and the molar extinction coefficient of the E113D mutant was higher than that of the wild type (119%) (Figure 2A and Table 1). (It should be noted that the values for the E113A/A117D, E113Q/A292E, and E113Q/A292D mutants might be underestimated because of the possible presence of the unprotonated form. Also, the values for the E113D and T94E/E113Q mutants contain some uncertainties because of the presence of isomers other than 11-*cis*-retinal in the binding pocket.) These results indicate that the extinction coefficient is finely tuned by the location of the counterion.

The reduced extinction coefficients resulted in the reduced photosensitivities of many of the mutants (61−81%) (Figure 4A and Table 2). However, oscillator strengths of those mutants were relatively similar to that of the wild type (84−100%) (Figure 2C and Table 1). These results indicate that the mutants might have a reduced photosensitivity for a single wavelength of light but

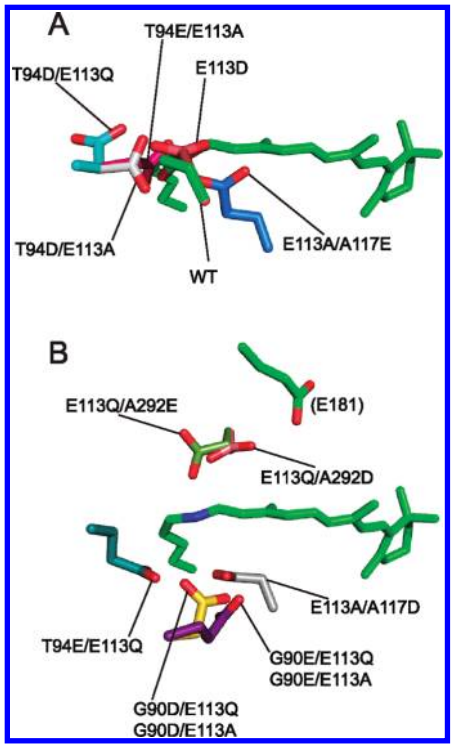

FIGURE 5: Locations of the counterion in the rhodopsin wild type and mutants inferred from molecular modeling. (A) Side chains of the counterion residues in the wild type and the mutants whose photosensitivity was 89−119% of that of the wild type and bandwidth was 100−106% of that of the wild type. (B) Side chains of the counterion residues in the mutants whose photosensitivity was 67−81% of that of the wild type and bandwidth was 118−133% of that of the wild type. E181 in the wild type is shown for reference.

a wild-type-like photosensitivity for light with a broad spectrum. Therefore, the counterion does not have to be located at position 113 for a high photosensitivity for natural light to exist.

Then why is E113 conserved as the counterion among vertebrate visual pigments? In other words, do the mutants function differently from the wild type in aspect(s) other than photosensitivity? First, it is known that the opsins (the chromophore-free state) of the G90D, T94D, and A292E mutants activate transducin (*23*), and their constitutive activity would desensitize the photoreceptor cell (*27*). The constitutive activity is thought to be caused by disruption of the salt bridge between K296 and

E113 (*28*). Although it is not known whether the double mutant opsins are constitutively active, this mechanism suggests that these double mutant opsins might also have constitutive activities. Second, all of the mutants but E113D exhibited ~100−10000-fold increased hydroxylamine sensitivity (Figure 4C and Table 2). Hydroxylamine sensitivity is a measure of Schiff base instability or accessibility from the bulk solution. Therefore, these results suggest that changing the position of the counterion destabilizes the Schiff base or increases its accessibility. The physiological consequences of Schiff base instability or increased accessibility are difficult to predict, but the resultant increase in the concentration of opsin that has a weak constitutive activity may desensitize the photoreceptor (*29*). Taken together, these findings suggest that the reason for the conservation of E113 as the counterion among vertebrate visual pigments may be that position 113 is the only position of the counterion that gives a low constitutive activity and a high Schiff base stability.

G protein activation by rhodopsin is another essential step that affects the efficiency of phototransduction. It is possible that counterion displacement alters the efficiency of formation of the active intermediate and/or the efficiency of activation of G protein by this intermediate. Although we have not measured the G protein activation ability of the mutants, Sakmar and colleagues reported that the E113D mutant (*5*), the E113A/A117E mutant (*22*), and the G90D/E113A mutant (*21*) exhibited reduced rates of G protein activation (0.89, ~0.7, and 0.43 relative to that of the wild type, respectively). However, we cannot conclude that these differences were due to the altered efficiency of the formation of the active intermediate and/or G protein activation efficiency because the amount of photoisomerized pigment was not precisely estimated in those studies.

Counterion Location and Bandwidth of the Absorption Spectrum. Another finding of this study is that the location of the counterion affects the bandwidth at half-maximum of the absorption spectrum. Interestingly, all of the mutants with a lower extinction coefficient (67−81%) had a broadened bandwidth (118−133%), whereas all of the mutants with a wild-type-like extinction coefficient (89−119%) had a wild-type-like bandwidth (100−106%). The results of the molecular modeling showed that counterions that are located approximately in the plane containing the 13-methyl groups and the Schiff base region of the chromophore give a wild-type-like extinction coefficient (89−119%) and a wild-type-like bandwidth (100−106%), whereas counterions that are located out of this plane give a lower extinction coefficient (67−81%) and a broader bandwidth (118−133%) (Figure 5). Although the mechanism is not clear, this will be a good subject for future quantum-chemical computational studies focusing on the mechanisms determining the absorption spectrum of rhodopsin.

Isomer Selectivity of the Binding Pocket and Photoisomerization. The isomer selectivity of the chromophore binding pocket and the bond specificity of the photoisomerization are important features of rhodopsin. HPLC analysis demonstrated that most of the mutants have an 11-*cis*-retinal chromophore that undergoes photoisomerization to all-*trans*-retinal, as in the case of the wild type. Therefore, the measured quantum yields equal the quantum yields of 11-*cis* to all-*trans* photoisomerization. However, there were two exceptions to this among the current mutants. In the T94E/E113Q mutant, all-*trans*-retinal was present (30%) along with 11-*cis*-retinal in the dark state. This fraction of all-*trans*-retinal might be associated with the unique shoulder around 400 nm in the absorption spectrum (Figure 1D). This observation, along with a previous report that the T94I mutant bound all-*trans*-retinal to form a pigment (*24*), suggests a possible role of position 94 in the isomer selectivity of the binding pocket. The chromatogram of the E113D mutant in the dark state contained an unassignable 15-*syn* peak and a peak apparently corresponding to 13-*cis*-15-*anti*-retinaloxime, along with peaks for 11-*cis*-retinal (Figure 3A,B). In addition, the photoreaction of E113D produced a substantial amount of 13-*cis*-retinal along with all-*trans*-retinal (Figure 3A). We speculate that the unassignable 15-*syn* peak and the peak that apparently corresponded to 13-*cis*-15-*anti*-retinaloxime in the dark state are derived from 15-*syn*- and 15-*anti*-retinaloximes of 11,13-*dicis*-retinal, respectively. The rationale for this speculation is as follows. First, it is unlikely that the 13-*cis*-retinal in the irradiated sample was directly generated by the two-double-bond photoisomerization of 11-*cis*-retinal, which can be reconciled by supposing that the 13-*cis*-retinal was generated by one-double-bond photoisomerization of either 7,13-*dicis*-retinal, 9,13-*dicis*-retinal, or 11,13-*dicis*-retinal. It has been shown or suggested that these *dicis*-retinals can be accommodated by the binding pocket (*25*). Second, the retention times of the 15-*syn*-retinaloximes of 7,13-*dicis*-retinal and 9,13-*dicis*-retinal have been reported and are different from that of the current unassignable 15-*syn* peak (*26*), suggesting that the unassignable 15-*syn* peak corresponds to 11,13-*dicis*-15-*syn*-retinaloxime. Finally, the given isomer of retinaloxime generally exists as a set of 15-*syn* and 15-*anti* forms. However, the counterparts of the unassignable 15-*syn*-retinaloxime and the 13-*cis*-15-*anti*-retinaloxime (i.e., 15-*anti*- and 15-*syn*-retinaloximes, respectively) were not found in the dark state. Therefore, it is natural to speculate that the counterpart (15-*anti*-retinaloxime) of the unassignable 15-*syn*-retinaloxime has a retention time identical to that of 13-*cis*-15-*anti*-retinaloxime, and that the peak apparently corresponding to the 13-*cis*-15-*anti*-retinaloxime in the dark state actually corresponds to the counterpart (15-*anti*-retinaloxime) of the unassignable 15-*syn*-retinaloxime. Then the corresponding peak in the irradiated sample would be derived from a mixture of 15-*anti*-retinaloximes of 13-*cis*-retinal and the unidentified isomer. Taking these together, we can speculate that the two peaks in the dark state are derived from 11,13-*dicis*-retinal bound to opsin. Then the 13-*cis*-retinal found in the irradiated sample should be generated by C11=C12 photoisomerization of 11,13-*dicis*-retinal, while the all-*trans*-retinal should be generated by C11=C12 photoisomerization of 11-*cis*-retinal. Although we cannot test our speculations because we do not have the authentic sample of 11,13-*dicis*-retinaloxime, we can safely say that the binding pocket of the E113D mutant has an altered preference for retinal isomers. Importantly, this might provide an explanation for the almost complete conservation of E, not D, at position 113 among vertebrate visual pigments. Understanding the mechanism would require some computational approaches.

Comparisons with Invertebrate Rhodopsins. Invertebrate rhodopsins have E181 rather than E113 as the Schiff base counterion (*9*). The quantum yields of the forward reaction in crayfish rhodopsin and octopus rhodopsin are 0.69 (*30*) and 0.69 ± 0.03 (*31*), respectively, which are similar to that of bovine rhodopsin, 0.65 (*19*). This is consistent with our finding that the counterion does not have to be located at position 113 to facilitate photoisomerization. On the other hand, the molar extinction coefficients of octopus rhodopsin (*32*), squid rhodopsin (*33*), and *Drosophila* Rh1 (*34*) at the respective λ_{max} are 27000 ± 3000, 35000 ± 1000, and 35000 ± 2700 M^{-1} cm^{-1}, respectively, which are slightly lower (67−86%) than that of bovine rhodopsin

[40600 M^{-1} cm^{-1} (*17*)]. In addition, the bandwidths at half-maximum of squid rhodopsin and octopus rhodopsin at −65 °C are reported to be 4270 and 4370 cm^{-1}, respectively (*35*), which are slightly larger (109 and 112%, respectively) than the value of bovine rhodopsin (3900 cm^{-1}) reported by the same group (*36*). Similarly, it is reported that the value of *Drosophila* Rh1 at 4 °C is 4700 cm^{-1} (*37*), which is 111% of the value of bovine rhodopsin (4220 cm^{-1}) reported by the same group (*38*). Although detailed experiments with the focus on the shape of absorption spectra of vertebrate and invertebrate rhodopsins are still necessary, the differences in extinction coefficient and bandwidth between vertebrate and invertebrate rhodopsins imply that the E181 counterion gives a smaller extinction coefficient and a broader bandwidth than E113. In fact, in the crystal structure of bovine rhodopsin (*20*) and squid rhodopsin (*39*), E181 is located out of the plane, that was inferred from the current molecular modeling (Figure 5B). It is not clear whether the difference in the bandwidth of the absorption spectrum between vertebrate and invertebrate rhodopsins would affect the functions of these pigments.

It is known that squid rhodopsin is stable to hydroxylamine (*40*). If this is universal for all of the rhodopsins with the E181 counterion, position 181, like position 113, might be a position for the counterion that allows a high stability of the Schiff base linkage. If so, is there any advantage of having the counterion at position 113 versus position 181? This is a key question for understanding the driving force of the displacement of the counterion from position 181 to position 113 in the course of opsin evolution (*9*). It has been suggested that efficiency of G protein activation was elevated by the counterion displacement (*9*). In this respect, it would be interesting to investigate properties such as constitutive activity of invertebrate rhodopsins.

ACKNOWLEDGMENT

We thank Dr. S. Koike for providing us with the HEK 293T cell line, Prof. F. Tokunaga for providing us with a pUSRα expression vector, and Prof. R. S. Molday for the generous gift of a Rho1D4-producing hybridoma. We are also grateful to Drs. Y. Imamoto and T. Yamashita for valuable discussions and Dr. E. Nakajima for her critical reading of our manuscript and invaluable comments.

REFERENCES

1. Kandori, H., Shichida, Y., and Yoshizawa, T. (2001) Photoisomerization in rhodopsin. *Biochemistry* (*Moscow, Russ. Fed.*) *66*, 1197–1209.
2. Shichida, Y., and Morizumi, T. (2006) Mechanism of G-protein activation by rhodopsin. *Photochem. Photobiol. 83*, 70–75.
3. Tsutsui, K., and Shichida, Y. (2010) Multiple functions of Schiff base counterion in rhodopsins. *Photochem. Photobiol. Sci. 9*, 1426–1434.
4. Zhukovsky, E. A., and Oprian, D. D. (1989) Effect of carboxylic acid side chains on the absorption maximum of visual pigments. *Science 246*, 928–930.
5. Sakmar, T. P., Franke, R. R., and Khorana, H. G. (1989) Glutamic acid-113 serves as the retinylidene Schiff base counterion in bovine rhodopsin. *Proc. Natl. Acad. Sci. U.S.A. 86*, 8309–8313.
6. Nathans, J. (1990) Determinants of visual pigment absorbance: Identification of the retinylidene Schiff's base counterion in bovine rhodopsin. *Biochemistry 29*, 9746–9752.
7. Tsutsui, K., Imai, H., and Shichida, Y. (2007) Photoisomerization efficiency in UV-absorbing visual pigments: Protein-directed isomerization of an unprotonated retinal Schiff base. *Biochemistry 46*, 6437–6445.
8. Tsutsui, K., Imai, H., and Shichida, Y. (2008) E113 is required for the efficient photoisomerization of the unprotonated chromophore in a UV-absorbing visual pigment. *Biochemistry 47*, 10829–10833.
9. Terakita, A., Koyanagi, M., Tsukamoto, H., Yamashita, T., Miyata, T., and Shichida, Y. (2004) Counterion displacement in the molecular evolution of the rhodopsin family. *Nat. Struct. Mol. Biol. 11*, 284–289.
10. Rao, V. R., Cohen, G. B., and Oprian, D. D. (1994) Rhodopsin mutation G90D and a molecular mechanism for congenital night blindness. *Nature 367*, 639–642.
11. al-Jandal, N., Farrar, G. J., Kiang, A. S., Humphries, M. M., Bannon, N., Findlay, J. B., Humphries, P., and Kenna, P. F. (1999) A novel mutation within the rhodopsin gene (Thr-94-Ile) causing autosomal dominant congenital stationary night blindness. *Hum. Mutat. 13*, 75–81.
12. Zhukovsky, E. A., Robinson, P. R., and Oprian, D. D. (1992) Changing the location of the Schiff base counterion in rhodopsin. *Biochemistry 31*, 10400–10405.
13. Zvyaga, T. A., Min, K. C., Beck, M., and Sakmar, T. P. (1993) Movement of the retinylidene Schiff base counterion in rhodopsin by one helix turn reverses the pH dependence of the metarhodopsin I to metarhodopsin II transition. *J. Biol. Chem. 268*, 4661–4667.
14. Dryja, T. P., Berson, E. L., Rao, V. R., and Oprian, D. D. (1993) Heterozygous missense mutation in the rhodopsin gene as a cause of congenital stationary night blindness. *Nat. Genet. 4*, 280–283.
15. Kayada, S., Hisatomi, O., and Tokunaga, F. (1995) Cloning and expression of frog rhodopsin cDNA. *Comp. Biochem. Physiol., Part B: Biochem. Mol. Biol. 110*, 599–604.
16. Imai, H., Terakita, A., and Shichida, Y. (2000) Analysis of amino acid residues in rhodopsin and cone visual pigments that determine their molecular properties. *Methods Enzymol. 315*, 293–312.
17. Wald, G., and Brown, P. K. (1953) The molar extinction of rhodopsin. *J. Gen. Physiol. 37*, 189–200.
18. Birge, R. R., Einterz, C. M., Knapp, H. M., and Murray, L. P. (1988) The nature of the primary photochemical events in rhodopsin and isorhodopsin. *Biophys. J. 53*, 367–385.
19. Kim, J. E., Tauber, M. J., and Mathies, R. A. (2001) Wavelength dependent cis-trans isomerization in vision. *Biochemistry 40*, 13774–13778.
20. Okada, T., Sugihara, M., Bondar, A. N., Elstner, M., Entel, P., and Buss, V. (2004) The retinal conformation and its environment in rhodopsin in light of a new 2.2 Å crystal structure. *J. Mol. Biol. 342*, 571–583.
21. Zvyaga, T. A., Fahmy, K., Siebert, F., and Sakmar, T. P. (1996) Characterization of the mutant visual pigment responsible for congenital night blindness: A biochemical and Fourier-transform infrared spectroscopy study. *Biochemistry 35*, 7536–7545.
22. Gross, A. K., Rao, V. R., and Oprian, D. D. (2003) Characterization of rhodopsin congenital night blindness mutant T94I. *Biochemistry 42*, 2009–2015.
23. Jin, S., Cornwall, M. C., and Oprian, D. D. (2003) Opsin activation as a cause of congenital night blindness. *Nat. Neurosci. 6*, 731–735.
24. Kim, J. M., Altenbach, C., Kono, M., Oprian, D. D., Hubbell, W. L., and Khorana, H. G. (2004) Structural origins of constitutive activation in rhodopsin: Role of the K296/E113 salt bridge. *Proc. Natl. Acad. Sci. U.S.A. 101*, 12508–12513.
25. Kefalov, V. J., Estevez, M. E., Kono, M., Goletz, P. W., Crouch, R. K., Cornwall, M. C., and Yau, K. W. (2005) Breaking the covalent bond: A pigment property that contributes to desensitization in cones. *Neuron 46*, 879–890.
26. Zvyaga, T. A., Fahmy, K., and Sakmar, T. P. (1994) Characterization of rhodopsin-transducin interaction: A mutant rhodopsin photoproduct with a protonated Schiff base activates transducin. *Biochemistry 33*, 9753–9761.
27. Ramon, E., del Valle, L. J., and Garriga, P. (2003) Unusual thermal and conformational properties of the rhodopsin congenital night blindness mutant Thr-94 → Ile. *J. Biol. Chem. 278*, 6427–6432.
28. Liu, R. S. H., and Mirzadegan, T. (1988) The shape of a three-dimensional binding site of rhodopsin based on molecular modeling analysis of isomeric and other visual pigment analogs. Bioorganic studies of visual pigments. 11. *J. Am. Chem. Soc. 110*, 8617–8623.
29. Trehan, A., Liu, R. S. H., Shichida, Y., Imamoto, Y., Nakamura, K., and Yoshizawa, T. (1990) On retention of chromophore configuration of rhodopsin isomers derived from three *dicis* retinal isomers. *Bioorg. Chem. 18*, 30–40.
30. Cronin, T. W., and Goldsmith, T. H. (1982) Quantum efficiency and photosensitivity of the rhodopsin equilibrium metarhodopsin conversion in crayfish photoreceptors. *Photochem. Photobiol. 36*, 447–454.
31. Dixon, S. F., and Cooper, A. (1987) Quantum efficiencies of the reversible photoreaction of octopus rhodopsin. *Photochem. Photobiol. 46*, 115–119.
32. Koutalos, Y., Ebrey, T. G., Tsuda, M., Odashima, K., Lien, T., Park, M. H., Shimizu, N., Derguini, F., Nakanishi, K., and Gilson, H. R.; et al. (1989) Regeneration of bovine and octopus opsins in situ with natural and artificial retinals. *Biochemistry 28*, 2732–2739.

33. Suzuki, T., Uji, K., and Kito, Y. (1976) Studies on cephalopod rhodopsin: Photoisomerization of the chromophore. *Biochim. Biophys. Acta 428*, 321–338.
34. Ostroy, S. E. (1978) Characteristics of *Drosophila* rhodopsin in wild-type and norpA vision transduction mutants. *J. Gen. Physiol. 72*, 717–732.
35. Kropf, A., Brown, P. K., and Hubbard, R. (1959) Lumi- and meta-rhodopsins of squid and octopus. *Nature 183*, 446–448.
36. Hubbard, R., Brown, P. K., and Kropf, A. (1959) Vertebrate lumi- and meta-rhodopsins. *Nature 183*, 442–446.
37. Vought, B. W., Salcedo, E., Chadwell, L. V., Britt, S. G., Birge, R. R., and Knox, B. E. (2000) Characterization of the primary photointermediates of *Drosophila* rhodopsin. *Biochemistry 39*, 14128–14137.
38. Vought, B. W., Dukkipatti, A., Max, M., Knox, B. E., and Birge, R. R. (1999) Photochemistry of the primary event in short-wavelength visual opsins at low temperature. *Biochemistry 38*, 11287–11297.
39. Murakami, M., and Kouyama, T. (2008) Crystal structure of squid rhodopsin. *Nature 453*, 363–367.
40. Hubbard, R., and St. George, R. C. C. (1958) The rhodopsin system of the squid. *J. Gen. Physiol. 41*, 501–528.